

---

# Inverse-Directed Propagation-Based Hexagonal Hogel Sampling for Holographic Stereogram Printing System

---

Anar Khuderchuluun<sup>1</sup>, Munkh-Uchral Erdenebat<sup>1</sup>,  
Erkhembaatar Dashdavaa<sup>1</sup>, Ki-Chul Kwon<sup>1</sup>,  
Jong-Rae Jeong<sup>2</sup> and Nam Kim<sup>1,\*</sup>

<sup>1</sup>*School of Information and Communication Engineering, Chungbuk National University, 1 Chungdaero, Seowongu, Cheongju, Chungbuk 28644, South Korea*

<sup>2</sup>*Department of Information and Communication, Suwon Science College, 288 Seja-ro, Jeongnam-myun, Hwaseong, Gyeonggi 18516, South Korea*  
*E-mail: namkim@chungbuk.ac.kr*

*\*Corresponding Author*

Received 16 November 2021; Accepted 24 February 2022;  
Publication 15 April 2022

## Abstract

Holographic stereogram (HS) printing is a promising holographic technique for three-dimensional (3D) visualization of an object with accurate depth cues. In this paper, unlike the conventional rectangular hogel based HS, efficient hexagonal hogels sampling for HS printing that enhances the volumetric visualization of reconstruction while providing rapidly generated data using inverse-directed propagation (IDP) is proposed. Specifically, an array of hexagonal hogels is sampled by a computer-generated integral imaging technique using an IDP, which acquires the full information of the 3D object prior to higher volumetric 3D reconstruction. To demonstrate the proposed

*Journal of Web Engineering, Vol. 21.4, 1225–1238.*

doi: 10.13052/jwe1540-9589.2149

© 2022 River Publishers

approach, IDP-based hexagonal hogel sampling for HS printing is implemented, and the enhanced image quality of printed holograms is verified both by numerical simulation and in an optical experiment.

**Keywords:** Holographic printer, holographic stereogram, computer-generated integral imaging, computer-generated hologram (CGH).

## 1 Introduction

Holography is advanced three-dimensional (3D) display technology that is predicted to supply all depth cues required by human eyes. Holography has improved rapidly and has many applications including 3D displays, holographic optical elements (HOEs), and hologram printing [1–4]. In recent years, holographic printing, a highly promising 3D imaging technique, has been used to represent realistic 3D scenes. The main feature of holographic printing is that the entire hologram consists of multiple sub-holograms (hogels), which are sequentially displayed on a spatial light modulator (SLM) and recorded on holographic material via an optical setup of holographic printing system [5–7]. Generally, holographic printing is classified into three types: holographic stereogram (HS) printing, wavefront printing, and holographic fringe printing. Among these three types, HS printing is commonly utilized in the field of holographic printing systems. This method reproduces 3D images of objects in a variety of sizes under incoherent illumination; texture, shading, reflections, and occlusion effects are created due to using a light-field rendering technique [8–11]. An efficient hogel-based HS synthesis approach is proposed for HS printing by decreasing spatial-angular trade-off [12]. Moreover, several HS methods based on integral imaging (InIm) techniques are presented by using fast Fourier transform (FFT) calculations to convert an elemental image (EI) into a hogel; this improves HS image quality [13, 14]. Also, a simplified fast HS method based on InIm [using the inverse-directed propagation (IDP) algorithm] has been applied for direct HS printing without degrading image quality [15].

In this paper, we present inverse-directed propagation-based hexagonal hogel sampling for an HS printing system. Hexagonal hogel sampling proceeds via IDP; this yields fully computed parameters for HS printing and enhances the solid 3D visualization because of the higher sampling density (despite simple and fast computation). The proposed IDP-based hexagonal hogel sampling method allows for effective HS printing.

## 2 Proposed Method

In this paper, IDP-based hexagonal hogel sampling for the HS printing system is proposed. Fully analyzed digital content is used to enhance 3D reconstruction. Figure 1 presents a schematic of IDP-based hexagonal hogel sampling for an HS printing system that yields a qualified 3D representation of an object. There are three major steps in the HS printing: initialization; IDP-based hexagonal hogel sampling [during which phase-modulated hexagonal hogels are generated]; and hexagonal hogel printing under a fully automated personal computer-based controller.

First, the initialization process is implemented to obtain color and depth data of the high-density 3D object by accessing depth layers. In addition, the main parameters for hexagonal elemental image (HEI) sampling, such as the details of the virtual hexagonal lens array (focal length, pitch of hexagonal elemental lenses, and number), gap ( $g$ ) from the HEI plane to the virtual hexagonal lens array, and pixel pitch of the HEI plane are optimized depending on the hogel printing setup. Then, the obtained 3D object data and optimized parameters are input to the second step for the asymmetrical structured hexagonal hogel array generation.

Secondly as shown in Figure 2, the IDP-based hexagonal hogel sampling is applied by using computer-generated integral imaging (CGII) based on the IDP algorithm [15] to acquire HEIs. In the HEI generation, a propagation direction of light is inverted from that of the HEI plane to that of the 3D object's point plane, based on IDP. Thus, the light propagations from all pixels of HEI pass through only the corresponding single hexagonal elemental lens.

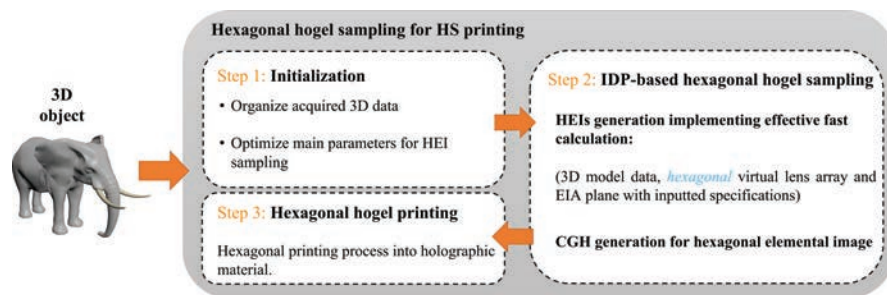


**Figure 1** Schematic of the proposed IDP-based hexagonal hogel sampling method for HS printing.

In contrast, in the conventional InIm method, each point of a 3D object is imaged by every elemental lens and directly stored as EI plane's pixels, where possible; the corresponding color data is re-stored at the corresponding pixels of the EI plane. This creates a double loop when checking that the computational conditions are satisfied during conventional EIA generation and lead to a computation time longer. Furthermore, hexagonal EIA generation is difficult using conventional InIm methods, because additional calculations are required to establish the nearest distance between an arbitrary HEI pixel and the center of each elemental lens [16]. In our method, the hexagonal EIA is sampled using the following equation:

$$u = x_{HLC} + (x_{HLC} - E_X) \frac{z}{g}, v = y_{HLC} + (y_{HLC} - E_Y) \frac{z}{g} \quad (1)$$

where  $x_{HLC}, y_{HLC}$  is the center of a hexagonal elemental lens and  $E_X$  and  $E_Y$  are the coordinates of a pixel on the HEI plane. If a point of a 3D object lies on the calculated point  $(u, v, z)$ , color data on that point is saved as an HEI pixel  $(E_X, E_Y)$ . There is no need to check all 3D object points for every elemental lens. The single HEI pixel is imaged via only the single corresponding lens, allowing for independent HEI generation that aids parallel computing. Thus, the computation iteration number is defined only by the resolution of the hexagonal EIA plane; this reduces computational time. In addition, the occlusion effect is easily included in calculation because (for example) if two object points, A and B, are defined for an HEI pixel (in Figure 2), the

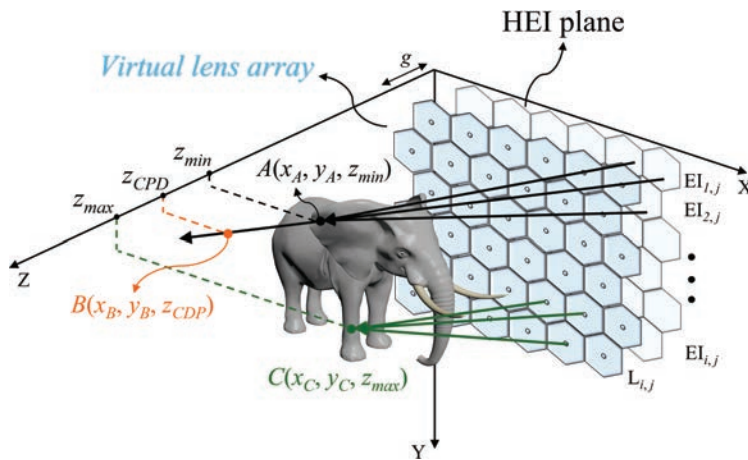


Figure 2 HEIs generation using IDP.

point nearest the HEI plane is stored at the HEI pixel. Hence, occlusion is considered without the need for an additional algorithm (e.g., the hidden point removal operator). After hexagonal EIA generation, each HEI is subjected to a single FFT to yield the hogel fringe pattern. Then, the hogel is calculated by integrating the fringe pattern with a reference beam. This allows for off-axis hologram generation via Fresnel propagation according to Equation (2), where  $z$  is the distance from the HEI plane to the hogel plane,  $(\xi, \eta)$  and  $(x, y)$  are the spatial coordinates at the hogel and reconstruction planes,  $k$  is the wavenumber,  $U_o(x, y)$  is the complex amplitude of HEI, and  $FFT$  and  $IFFT$  the Fourier and inverse Fourier transform operators, respectively.

$$U_{hogel}(\xi, \eta) = \frac{e^{jkz}}{j\lambda z} IFFT \left[ FFT[U_o(x, y)] \times FFT \left[ \exp \left( j \frac{k}{2z} (x^2 + y^2) \right) \right] \right] \quad (2)$$

Most HS printing systems employ rectangular hogel sampling; the light propagation distribution is sampled by a rectangular lattice. However, when a hexagonal lens array is sampled, the volumetric visualization (which is including a parallax, occlusion, and depth information) of a reconstructed 3D object is higher compared to that after sampling using a conventional rectangular lens array because the sampling density of the former array is larger. This is widely used in InIm systems to enhance 3D image quality [17–19]. More hexagonal than rectangular elemental lenses fit into the same area  $S$ ; the pitches of all elemental lenses are denoted by  $P$  (Figure 3). Also, a single hexagonal elemental lens is neighbored by six hexagonal elemental lenses at the same distances; a single rectangular elemental lens is neighbored by only four elemental lenses. Thus, hexagonal hogel sampling has a higher fill factor than conventional rectangular hogel-based sampling; this enhances volumetric 3D visualization. Note that, the fill factor is evaluated by the ratio of areas covered by elemental lenses to a total area of the elemental lens array. In addition, the spatial resolution of the 3D reconstruction is enhanced accordingly due to the higher sampling rate of the hexagonal sampling.

Finally, fully automatic hexagonal hogel printing employing a graphical user interface (GUI) is implemented. A schematic of the optical setup for the hexagonal HS printing system is shown in Figure 4. The SLM, X-Y translation stage, and electrical shutter are synchronously controlled by a personal computer (PC). The hogel printing path creates an asymmetrical, structured hexagonal hogel array. The hogels are sequentially printed.

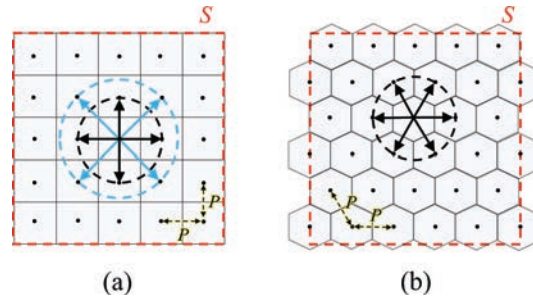


**Figure 3** Sampling structures of the lens arrays: (a) The rectangular lens array, (b) The hexagonal lens array.

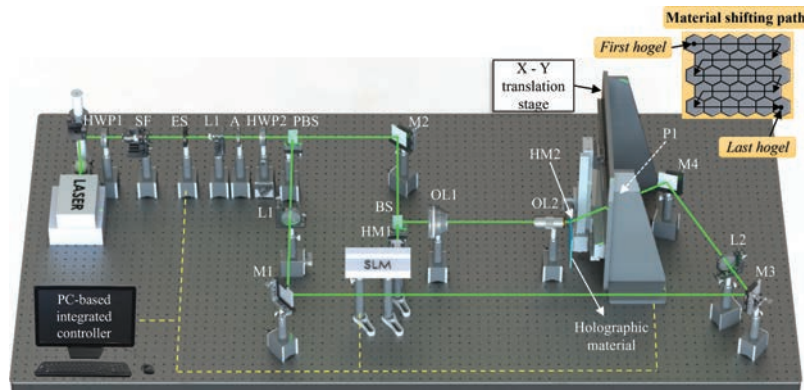


**Figure 4** Schematic of hexagonal hogel-based HS printing and the material shifting path (X-Y translation).

### 3 Simulation and Experimental Result

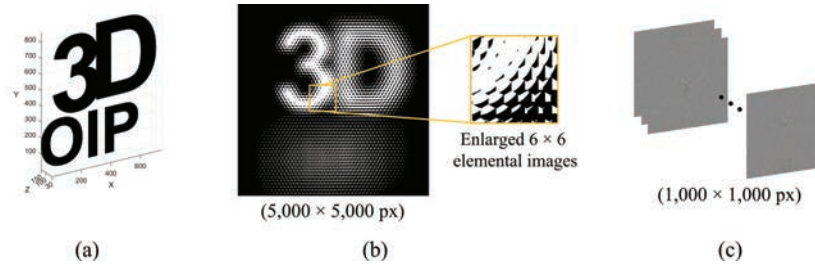
In the experiment, a simple virtual 3D object was used. The digital content for the hexagonal hogels was generated as quickly as possible with enhancement of 3D image quality. The computer-generated data on hexagonal hogels were printed on holographic material optically. The experimental results afforded by IDP-based, hexagonal hogel HS printing prototype verified that 3D volume reconstruction was improved.

#### 3.1 IDP-based Hexagonal Hogel Sampling

HEIs were generated via IDP-based hexagonal hogel sampling from the object “3D OIP”. Table 1 demonstrates the details of optimized parameters in

**Table 1** Specifications of 3D object and main experimental parameters

Parameter	Details
HS resolution	$50,000 \times 50,000$ pixels
Phase-modulated hogel resolution	$1,000 \times 1,000$ pixels
Hexagonal hogel number	$58 \times 50$
Hexagonal lens array	$58 \times 50$ hexagonal elemental lenses Focal length: 3.3 mm Elemental lens pitch ( $P$ ): 1 mm
Hexagonal EIA plane resolution	$5,000 \times 5,000$ pixels (with 0.01 mm pixel pitch)
HEI resolution	$115 \times 100$ pixels
3D object	3D OIP (1,023,120 object points)
Personal computer	CPU: Intel(R) Core (TM) i7-8700 @ 3.2 GHz RAM: 16 GB GPU: NVIDIA GeForce GTX 1080Ti.

**Figure 5** IDP-based hexagonal hogel sampling. (a) The 3D point cloud object “3D OIP”. (b) The hexagonal EIA. (c) The phase-modulated HEIs (hexagonal hogels for HS printing).

the experiment, including the simple characters (number/letters) “3D OIP”, the main parameters required for HEI sampling, and the PC specifications.

The simple 3D object “3D OIP” and corresponding hexagonal EIA (produced using the parameters in Table 1) are presented in Figures 5(a) and 5(b) respectively. The phase-modulated hexagonal hogels for HS printing are shown in Figure 5(c).

Hexagonal EIA generation required only 2.08 s and IDP-based hexagonal hogel generation improved image quality. The CGH calculation time for  $58 \times 50$  phase-modulated hogels was 629.88 s via GPU parallel computing. Therefore, the total calculation time required to generate the digital data of the hexagonal hogels was approximately 631.96 s for a high-resolution hologram.

### 3.2 Hexagonal Hogel Printing

Hexagonal hogel-based HS printing, using the configuration in Figure 4, was implemented using the optimized hexagonal array structure. The prototype of hexagonal hogel-based HS printing system used the green laser with 532 nm wavelength, HOLOEYE LETO reflective-type phase-only SLM with  $1920 \times 1080$  pixels resolution and  $6.4 \mu\text{m}$  pixel pitch, and Litiholo CRT20 film which has  $16 \mu\text{m}$  thickness as a printing material. The generated CGH patterns for hogels were displayed on the SLM and illuminated by the object beam; these were then demagnified by the objective lenses and recorded to the holographic material within the reference beam illuminated from the opposite side of the material at  $45^\circ$  degrees.

The elementary hexagonal holograms are created one by one on the holographic film by following the material shifting path. In the hexagonal hogel printing,  $58 \times 50$  hexagonal hogels were successfully recorded on the area of  $50 \text{ mm}^2$  film where the size of each hexagonal hogel was  $1.15 \text{ mm} \times 1 \text{ mm}$  [Figure 6(a)]. Note that, the area of  $50 \text{ mm}^2$  film can occupy to record  $50 \times 50$  rectangular hogels. The intensity ratio of the two beams was 1:1 (4.5 mW) and the total printing time was approximately 2.41 hours where a hogel exposure time was 2 seconds, and a settling time was 1 second.

More hexagonal hogels are sampled and recorded when the hogels are uniformly distributed; in a single hexagonal hogel, there are six neighboring hogels with equal distances between lens centers. The  $6 \times 5$  hexagonal hogels and  $5 \times 5$  rectangular hogels are contained in the  $S$  area [Figures 6(a) and 6(b)], and the fill factors measured as 72.96% (rectangular hogel array) and 94.17% (hexagonal hogel array) in the printed hexagonal hogels and rectangular hogels respectively. As a result, the filter factor is enhanced by 1.29 times in the proposed hexagon hogel sampling compared to the rectangular

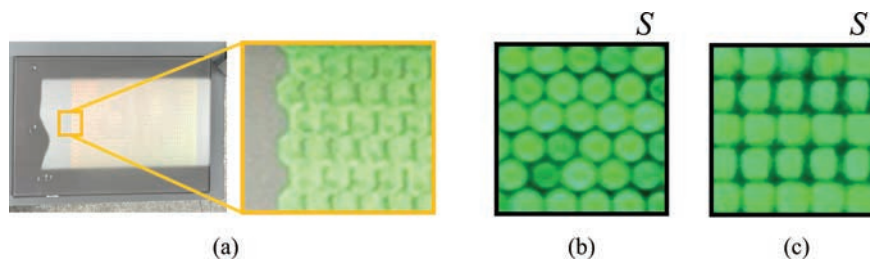


**Figure 6** Hogels printed on holographic material: (a) enlarged image of  $58 \times 50$  hexagonal hogels. (b) Reconstructions of  $6 \times 5$  hexagonal hogels and (c)  $5 \times 5$  rectangular hogels focused on the film.

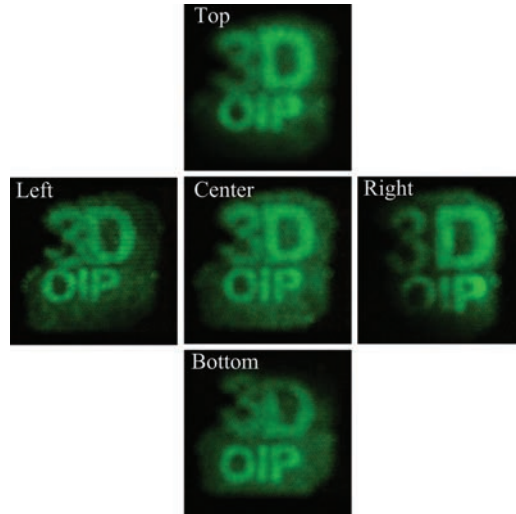


**Figure 7** Reconstructed images of the printed hexagonal hogel-based HS from different viewing positions.

hogel sampling. The reconstructed 3D images of the printed hexagonal hogel-based HS for the object “3D OIP” (from different viewpoints) under white light illumination are shown in Figure 7. The field of view (FOV) of the 3D reconstruction was approximately  $15^\circ$  in both horizontal and vertical axes.

#### **4 Conclusion**

We used IDP-based hexagonal hogels for HS printing; this allows for accurate and solid 3D visualization. Hexagonal hogels are sampled using an effective high-density sampling structure (a hexagonal grid) to create full-parallax HSs that were then recorded on holographic material using a hexagonal hogel printing system. Full-parallax 3D reproduction of the object was successful. Moreover, hexagonal hogel printing improved HS reconstruction by enhancing the fill factor and volumetric visualization of reconstruction more so than conventional rectangular hogel printing.

#### **Acknowledgments**

This work was supported by the National Research Foundation of Korea (NRF) grants funded by the Korean government (nos. NRF-2020R1A2C110

1258 & NRF-2018R1D1A3B07044041) and the Technology Development Program (grant no. S3058848) funded by the Ministry of SMEs and Startups (MSS, Korea).

## References

- [1] M.-U. Erdenebat, Y.-T. Lim, K.-C. Kwon, N. Darkhanbaatar, and N. Kim, 'Waveguide-type head-mounted display system for AR application', in *State of the Art Virtual Reality and Augmented Reality Knowhow* (IntechOpen), Chap. 4, 2018.
- [2] H.-Y. Wu, C.-W. Shin, and N. Kim, 'Full-color holographic optical elements for augmented reality display', in *Holographic Materials and Applications* (IntechOpen), Chap. 3, 2019.
- [3] C. W. Shin, H. Y. Wu, K. C. Kwon, Y. L. Piao, K. Y. Lee, S. K. Gil, and N. Kim, 'Diffraction efficiency enhancement and optimization in full-color HOE using the inhibition characteristics of the photopolymer', *Optics Express*, vol. 29, pp. 1175–1187, Jan. 2021.
- [4] N. Darkhanbaatar, M.-U. Erdenebat, C.-W. Shin, K.-C. Kwon, K.-Y. Lee, G. Baasantseren, and N. Kim, 'Three-dimensional see-through augmented-reality display system using a holographic micromirror array', *Appl. Opt.*, vol. 60, pp. 7545–7551, 2021.
- [5] H. Yoshikawa and M. Tachinami, 'Development of direct fringe printer for computer-generated holograms', *Proc. SPIE 5742*, 259, 2005.
- [6] T. Yamaguchi, O. Miyamoto, and H. Yoshikawa, 'Volume hologram printer to record the wavefront of three-dimensional objects', *Opt. Eng.* 51(7), 075802, 2012.
- [7] H. Kang, E. Stoykova, J. Park, S. Hong, and Y. Kim, 'Holographic printing of white-light viewable holograms and stereograms', in *Holography – Basic Principles and Contemporary Applications*, E. Mihaylova ed. (InTech), 2013.
- [8] J. Park, H. Kang, E. Stoykova, Y. Kim, S. Hong, Y. Choi, Y. Kim, S. Kwon, and S. Lee, 'Numerical reconstruction of a full parallax holographic stereogram with radial distortion', *Opt. Express* 22, pp. 20776–20788, 2014.
- [9] A. M. Sánchez and D. V. Prieto, 'Design, development, and implementation of a low-cost full-parallax holoprinter', *Proc. SPIE 10558*, 105580H, 2018.

- [10] E. Dashdavaa, A. Khuderchuluun, C.-W. Shin, Y.-T. Lim, and N. Kim, 'Holographic stereogram printer for computer-generated holograms', *Proc. SPIE* 10679, 106790V, 2018.
- [11] E. Dashdavaa, A. Khuderchuluun, Y.-T. Lim, S.-H. Jeon, and N. Kim, 'Holographic stereogram printing based on digitally computed content generation platform', *Proc. SPIE* 10944, 109440M, 2019.
- [12] E. Dashdavaa, A. Khuderchuluun, H.-Y. Wu, Y.-T. Lim, C.-W. Shin, H. Kang, S.-H. Jeon, and N. Kim, 'Efficient hogel-based hologram synthesis method for holographic stereogram printing', *Appl. Sci.* 10(22), pp. 2076–3417, 2020.
- [13] Z. Wang, R. S. Chen, X. Zhang, G. Q. Lv, Q. B. Feng, Z. A. Hu, H. Ming, and A. T. Wang, 'Resolution enhanced holographic stereogram based on integral imaging using moving array lenslet technique', *Appl. Phys. Lett.* 113, 221109, 2018.
- [14] P. Dai, G. Lv, Z. Wang, X. Zhang, X. Gong, and Q. Feng, 'Resolution-enhanced holographic stereogram based on integral imaging using a moving array lenslet technique and an aperture array filter', *Appl. Opt.*, vol. 58(30), pp. 8207–8212, 2019.
- [15] A. Khuderchuluun, Y.-Ling. Piao, M.-U. Erdenebat, E. Dashdavaa, M.-H. Lee, S.-H. Jeon, and N. Kim, 'Simplified digital content generation based on an inverse-directed propagation algorithm for holographic stereogram printing', *Appl. Opt.* 60(14), pp. 4235–4244, 2021.
- [16] D. H. Kim, J. W. Lee, J. S. Jeong, K. C. Kwon, K. H. Yoo, K. A. Kim, M. U. Erdenebat, and N. Kim, 'Real-time 3D display system based on computer-generated integral imaging technique using enhanced ISPP for hexagonal lens array', *Appl. Opt.* 52, pp. 8411–8418, 2013.
- [17] N. Chen and J. Yeom, J.-H. Park, and B. Lee, 'High resolution Fourier hologram generation using hexagonal lens array based on integral imaging', in *International Meeting on Information Display (Korean Information Display Society)*, pp. 729–730, 2011.
- [18] N. Chen, J. Yeom, J.-H. Jung, J.-H. Park, and B. Lee, 'Resolution comparison between integral-imaging-based hologram synthesis methods using rectangular and hexagonal lens arrays', *Opt. Express* 19, pp. 26917–26927, 2011.
- [19] J. Wen, X. Yan, X. Jiang, Z. Yan, Z. Wang, S. Chen, M. Lin, 'Comparative study on light modulation characteristic between hexagonal and rectangular arranged macro lens array for integral imaging based light field display', *Opt. Commun.*, 466, 125613, 2020.

## Biographies



**Anar Khuderchuluun** received her B.S. degree in Electronics and Automation Engineering from the National University of Mongolia in 2016. In 2017, she started an integrated MSc and DSc course that will culminate in a DSc degree in information and communication engineering from Chungbuk National University, Cheongju, South Korea. Her research interests include 3D imaging and computer-generated holograms, holographic printers, and HOE fabrication.



**Munkh-Uchral Erdenebat** received the M.S. and Ph.D. degrees in information and communication engineering from Chungbuk National University, Cheongju, South Korea, in 2011 and 2015, respectively. He is currently a Postgraduate Doctor Researcher with the School of Information and Communications Engineering, Chungbuk National University. His research interests include three-dimensional (3-D) displays and microscopy based on integral imaging and holographic techniques, 3-D image processing, 360° viewable displays, and light-field techniques.



**Erkhembaatar Dashdavaa** received his M.S. degree in Information and Communication Engineering from Chungbuk National University, Cheongju, South Korea. He is currently a Ph.D. candidate at the School of Information and Communication Engineering, Chungbuk National University since 2016. His research interests include digital holographic techniques and holographic printer especially holographic stereogram-based and wavefront-based printer, HOE fabrication.



**Ki-Chul Kwon** received a Ph.D. degree in information and communication engineering from Chungbuk National University, Cheongju, South Korea, in 2005. From 2008 to 2012, he was a Researcher for the BK21 Program with the College of Electrical and Computer Engineering, Chungbuk National University. He is the Research Professor of Electrical and Computer Engineering with the School of Information and Communications Engineering, Chungbuk National University. His research interest includes eye surgery using a microscope three-dimensional visualization system, medical image processing, and computer vision.



**Jong-Rae Jeong** received B.S and M.S degrees in electronics engineering from Yonsei University in 1982 and 1984 respectively. He received a Ph.D. degree in the graduate school of electronics engineering from Kyung Hee University in 2005. From 1983–1992, he was a senior researcher at the Samsung Electronics Co., Ltd. Information and Communication Research Institute. Since 1992, he has been a Professor with the department of Smart IT at Suwon Science College. His research interest includes optical signal processing, optical communication, network, mobile telecommunication, IoT, etc.



**Nam Kim** received a Ph.D. degree in electronic engineering from Yonsei University, Seoul, South Korea, in 1988. Since 1989, he has been a Professor with the School of Information and Communication Engineering, Chungbuk National University, Cheongju, South Korea. From 1992 to 1993, he was a Visiting Researcher with Dr. Goodman's Group, Stanford University. In addition, he attended Caltech as a Visiting Professor from 2000 to 2001. His research interests include the three-dimensional (3-D) display and visualization systems, 3-D medical imaging systems, 3-D image processing and applications based on stereoscopic, holography, and integral imaging techniques, diffractive optics, and optical security systems.